Dual-Localized Enzymatic Components Constitute the Fatty Acid Synthase Systems in Mitochondria and Plastids[1][OPEN]

Xin Guan,[a,b] Yozo Okazaki,[c,2] Rwisdom Zhang,[b,d] Kazuki Saito,[c,e] and Basil J. Nikolau[a,b,f,3,4]

[a]Roy J. Carver Department of Biochemistry, Biophysics, and Molecular Biology, Iowa State University, Ames, Iowa 50011
[b]Engineering Research Center for Biorenewable Chemicals, Iowa State University, Ames, Iowa 50011
[c]Metabolomics Research Group, RIKEN Center for Sustainable Resource Science, Yokohama 230–0045, Japan
[d]Department of Chemical Engineering, University of Southern California, Los Angeles, California 90007
[e]Graduate School of Pharmaceutical Sciences, Chiba University, Chiba 260–8675, Japan
[f]Center for Metabolic Biology, Iowa State University, Ames, Iowa 50011

ORCID IDs: 0000-0002-7983-2103 (X.G.); 0000-0002-4310-8519 (Y.O.); 0000-0001-6310-5342 (K.S.); 0000-0002-4672-7139 (B.J.N.)

Plant fatty acid biosynthesis occurs in both plastids and mitochondria. Here, we report the identification and characterization of Arabidopsis (*Arabidopsis thaliana*) genes encoding three enzymes shared between the mitochondria- and plastid-localized type II fatty acid synthase systems (mtFAS and ptFAS, respectively). Two of these enzymes, β-ketoacyl-acyl carrier protein (ACP) reductase and enoyl-ACP reductase, catalyze two of the reactions that constitute the core four-reaction cycle of the FAS system, which iteratively elongates the acyl chain by two carbon atoms per cycle. The third enzyme, malonyl-coenzyme A:ACP transacylase, catalyzes the reaction that loads the mtFAS system with substrate by malonylating the phosphopantetheinyl cofactor of ACP. GFP fusion experiments revealed that the these enzymes localize to both chloroplasts and mitochondria. This localization was validated by characterization of mutant alleles, which were rescued by transgenes expressing enzyme variants that were retargeted only to plastids or only to mitochondria. The singular retargeting of these proteins to plastids rescued the embryo lethality associated with disruption of the essential ptFAS system, but these rescued plants displayed phenotypes typical of the lack of mtFAS function, including reduced lipoylation of the H subunit of the glycine decarboxylase complex, hyperaccumulation of glycine, and reduced growth. However, these latter traits were reversible in an elevated-CO_2 atmosphere, which suppresses mtFAS-associated photorespiration-dependent chemotypes. Sharing enzymatic components between mtFAS and ptFAS systems constrains the evolution of these nonredundant fatty acid biosynthetic machineries.

In plants, de novo fatty acid biosynthesis occurs in two distinct subcellular compartments, the plastids and mitochondria (Ohlrogge and Jaworski, 1997; Wada et al., 1997). These two fatty acid biosynthetic systems utilize an acyl carrier protein (ACP)-dependent, multicomponent type II fatty acid synthase (FAS) to catalyze the assembly of these essential cellular components. Furthermore, genetic studies indicate that these two FAS systems are not redundant and have been evolutionarily retained (Guan et al., 2017). The plastid-produced fatty acids serve as the acyl building blocks for the assembly of the majority of the lipids in plant cells, including membrane lipids, signaling lipids, and storage lipids (Li-Beisson et al., 2013). In comparison, the primary role of mitochondrial FAS (mtFAS) is to synthesize the acyl precursor for the biosynthesis of lipoic acid (Yasuno and Wada, 1998; Wada et al., 2001a), which is the cofactor essential for the catalytic competence of several key metabolic enzymes, including the glycine decarboxylase complex (GDC), mitochondrial pyruvate dehydrogenase, α-ketoglutarate dehydrogenase (KGDH), branched-chain α-ketoacid dehydrogenase (BCKDH; Taylor et al., 2004), and plastidial pyruvate dehydrogenase (ptPDH; Wada et al., 2001b; Yasuno and

[1]This work was supported by the National Science Foundation (grant nos. IOS1139489, EEC0813570, and MCB0820823 to B.J.N.), the State of Iowa, the Japan Science and Technology Agency Strategic International Collaboration Research Program, and RIKEN Pioneering Project Integrated Lipidology.

[2]Present address: Graduate School of Bioresources, Mie University, Tsu City, Mie 514–8507, Japan.
[3]Author for contact: dimmas@iastate.edu.
[4]Senior author.

The author responsible for distribution of materials integral to the findings presented in this article in accordance with the policy described in the Instructions for Authors (www.plantphysiol.org) is: Basil J. Nikolau (dimmas@iastate.edu).

X.G. and B.J.N. designed the research; Y.O. and K.S. analyzed the lipidome; X.G. and R.Z. performed the in vitro enzymatic assays; X.G. and B.J.N. carried out all other experiments; X.G. and B.J.N. coordinated the preparation of the article; all authors contributed to the analysis of the collected data and writing of the article.

[OPEN]Articles can be viewed without a subscription.

www.plantphysiol.org/cgi/doi/10.1104/pp.19.01564

Wada, 2002). In addition, mtFAS appears to be involved in remodeling mitochondrial cardiolipins (Frentzen and Griebau, 1994; Griebau and Frentzen, 1994) and in detoxifying free malonic acid (Guan and Nikolau, 2016), a competitive inhibitor of succinate dehydrogenase of the tricarboxylic acid cycle (Quastel and Wooldridge, 1928; Greene and Greenamyre, 1995).

Detailed biochemical characterizations, going back to the 1980s, have led to the identification of the four enzymatic components of the core plastidic FAS (ptFAS) system: three isozymes of 3-ketoacyl-ACP synthases, a 3-ketoacyl-ACP reductase, a 3-hydroxyacyl-ACP dehydrase, and an enoyl-ACP reductase (ptER). In contrast, the enzymatic components of the mtFAS system are less well characterized. To date, only two of the core enzymatic components of the plant mtFAS system have been characterized, β-ketoacyl-ACP synthase (mtKAS; Olsen et al., 2004; Yasuno et al., 2004; Ewald et al., 2007) and 3-hydroxyacyl-ACP dehydratase (mtHD; Guan et al., 2017), along with the three mtACP isoforms that carry the intermediates of the mtFAS system (Fu et al., 2020). Other characterized supportive components of the mtFAS system include the mitochondrial phosphopantetheinyl transferase (mtPPT) that activates mtACP by phosphopantetheinylation (Guan et al., 2015) and malonyl-CoA synthetase (mtMCS) that generates the malonyl-CoA precursor for mtFAS (Guan and Nikolau, 2016). These more recent characterizations of the mtFAS system establish that whereas the ptFAS system uses acetyl-CoA, generated by the ptPDH, as the precursor for fatty acid biosynthesis, mtFAS uses malonyl-CoA as the precursor, which is generated by mtMCS (Guan and Nikolau, 2016).

Here, we report the identification and characterization of three additional enzymatic components of mtFAS that have not previously been identified. Two of these catalyze core reactions of the mtFAS cycle, namely β-ketoacyl-ACP reductase (KR) and enoyl-ACP reductase (ER), and the third is the mitochondrial malonyl-CoA:ACP transacylase (MCAT), which loads the mtFAS system by malonylating the phosphopantetheinyl cofactor of ACP. Unexpectedly, genetic and transgenic expression of fluorescently tagged proteins indicate that these three enzymatic components are shared between the mtFAS and ptFAS systems.

RESULTS

Computational Identification of Candidate Genes Encoding mtFAS Catalytic Components

BLAST analysis of the Arabidopsis (*Arabidopsis thaliana*) genome using the sequences of the yeast (*Saccharomyces cerevisiae*) mtFAS components and *Escherichia coli* FAS components as queries identified putative Arabidopsis open reading frames (ORFs) coding for mitochondrial MCAT, KR, and ER catalytic components (Supplemental Fig. S1). These analyses identified a single candidate gene each for mitochondrial MCAT (AT2G30200; Bryant et al., 2011) and KR (AT1G24360; Bryant et al., 2011) and two potential candidate genes for mitochondrial ER (AT3G45770 and AT2G05990; Mou et al., 2000; Wu et al., 2015). The sequences of these candidate proteins were most similar in the Arabidopsis proteome identified in TAIR10 (www.arabidopsis.org), as indicated by BLAST e-value scores of between 10^{-15} and 10^{-68}, and these proteins share between 20% and 45% sequence identity with the query sequences (Supplemental Fig. S1). Prior characterizations have indicated that all but AT3G45770 encode components of the ptFAS system (Mou et al., 2000; Bryant et al., 2011; Wu et al., 2015), and computational analyses suggest that AT3G45770 encodes a mitochondria-localized ER component (Li-Beisson et al., 2010, 2013).

Organelle Targeting of Candidate mtFAS Components

Because prior studies of these candidate mtFAS genes have indicated that they may be components of the ptFAS system (Mou et al., 2000; Bryant et al., 2011; Wu et al., 2015), initial characterizations directly evaluated whether these putative mtFAS component enzymes are mitochondrially located. Transgenic experiments were conducted with GFP-fusion proteins, expressed under the transcriptional regulation of the cauliflower mosaic virus 35S promoter (Fig. 1). Three types of GFP-fusion transgenes were evaluated for each of the candidate mtFAS component proteins: (1) GFP was translationally fused at the C terminus of each candidate mtFAS component protein; (2) the N-terminal segment from each candidate mtFAS component protein that was computationally predicted to be an organelle-targeting presequence was translationally fused to the N terminus of GFP; and (3) GFP was translationally fused at the C terminus of each candidate mtFAS component protein lacking the putative organelle-targeting presequence. Individual GFP-fusion transgenes were stably integrated into the Arabidopsis genome, and confocal micrographs of the resulting transgenic roots and leaves visualized the subcellular locations of the GFP-fusion proteins.

In these experiments, organelles were identified by a combination of two fluorescence markers: (1) MitoTracker Orange for mitochondria and chlorophyll autofluorescence for plastids; and (2) the fluorescence signals revealed by the expression of control GFP-tagged markers, the *p35S::mtPPT*$_{1\text{-}240}$*-GFP* transgene (Fig. 1A) that we previously identified as being targeted to mitochondria (Guan et al., 2015) and the *p35S::UGP3*$_{1\text{-}600}$*-GFP* transgene that is plastid targeted (Okazaki et al., 2009; Fig. 1A). These control markers show distinct patterns that are consistent with mitochondrial or plastid localization, and these are distinct from the GFP signal observed with the nontargeted GFP control, which, as previously characterized (Li et al., 2011a), is located in the cytosol and nucleus (Fig. 1A).

The fluorescence observed in transgenic plants carrying C-terminal GFP fusions with each full-length candidate

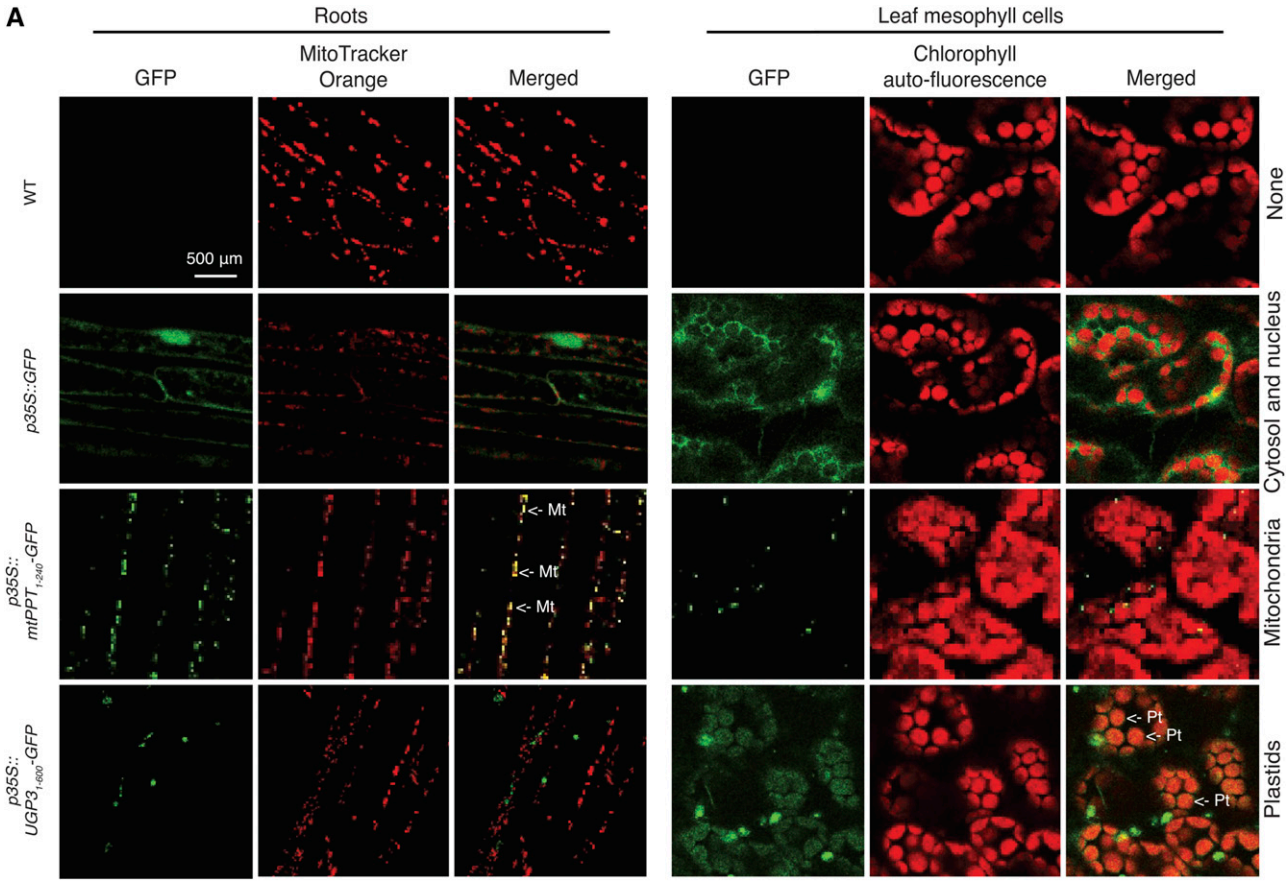

Figure 1. Subcellular localization of potential mtFAS proteins. Shown are confocal fluorescence micrographs of roots and leaf mesophyll cells, imaging the emission of GFP, MitoTracker Orange, chlorophyll autofluorescence, and the merged images. Fluorescence micrographs are from nontransgenic wild-type control plants (WT) and transgenic plants carrying the *p35S::GFP* control, *p35S::mtPPT*$_{1\text{-}240}$*-GFP*, or *p35S::UGP3*$_{1\text{-}600}$*-GFP* transgenes (A); *p35S::mtER*$_{1\text{-}1122}$*-GFP*, *p35S::mtER*$_{1\text{-}300}$*-GFP*, or *p35S::mtER*$_{301\text{-}1122}$*-GFP* transgenes (B); *p35S::pt/mtMCAT*$_{1\text{-}1179}$*-GFP*, *p35S::pt/mtMCAT*$_{1\text{-}216}$*-GFP*, or *p35S::pt/mtMCAT*$_{205\text{-}1179}$*-GFP* transgenes (C); *p35S::pt/mtKR*$_{1\text{-}957}$*-GFP*, *p35S::pt/mtKR*$_{1\text{-}234}$*-GFP*, or *p35S::pt/mtKR*$_{214\text{-}957}$*-GFP* transgenes (D); and *p35S::pt/mtER*$_{1\text{-}1167}$*-GFP*, *p35S::pt/mtER*$_{1\text{-}261}$*-GFP*, or *p35S::pt/mtER*$_{262\text{-}1167}$*-GFP* transgenes (E).

mtFAS component protein showed an assortment of organelle localizations. The interpretation of these results can be simplified if one considers that subcellular targeting information is segregated between both the N-terminal, potential organelle-targeting segment and the mature segment of each protein. This was particularly the case for the proteins encoded by AT2G05990, AT2G30200, and AT1G24360. The full-length proteins encoded by these three genes guide the expression of the fused GFP to both mitochondria and plastids (Fig. 1, C–E). In the case of the AT2G05990-encoded protein, the N-terminal presequence directs GFP to plastids (row 2 of Fig. 1E) but the segment that lacks this N-terminal presequence guides GFP to mitochondria (row 3 of Fig. 1E). In contrast, the N-terminal presequences of AT2G30200 and AT1G24360 direct the GFP fusions to mitochondria (row 2 of Fig. 1, C and D), whereas upon removal of these N-terminal presequences from each protein, the remaining mature segments direct the accumulation of the fused GFP protein to plastids (row 3 of Fig. 1, C and D).

Subcellular targeting information of the AT3G45770-encoded protein is simpler to interpret, with the full-length AT3G45770 protein (row 1 of Fig. 1B) and the N-terminal presequence (row 2 of Fig. 1B) directing GFP to mitochondria, whereas removal of the N-terminal presequence from the AT3G45770-encoded protein guides GFP to the cytosol (row 3 of Fig. 1B). In summary, therefore, in contrast to the AT3G45770-encoded protein, proteins encoded by AT2G30200, AT1G24360, and AT2G05990 encode dual-localization signals, for both mitochondria and plastids. One of these signals resides in the N-terminal presequence and the other in the mature portion of these proteins.

Experimental Authentication of Candidate mtFAS Component Enzymes

The catalytic functions of the individual putative FAS component proteins were explored via two independent

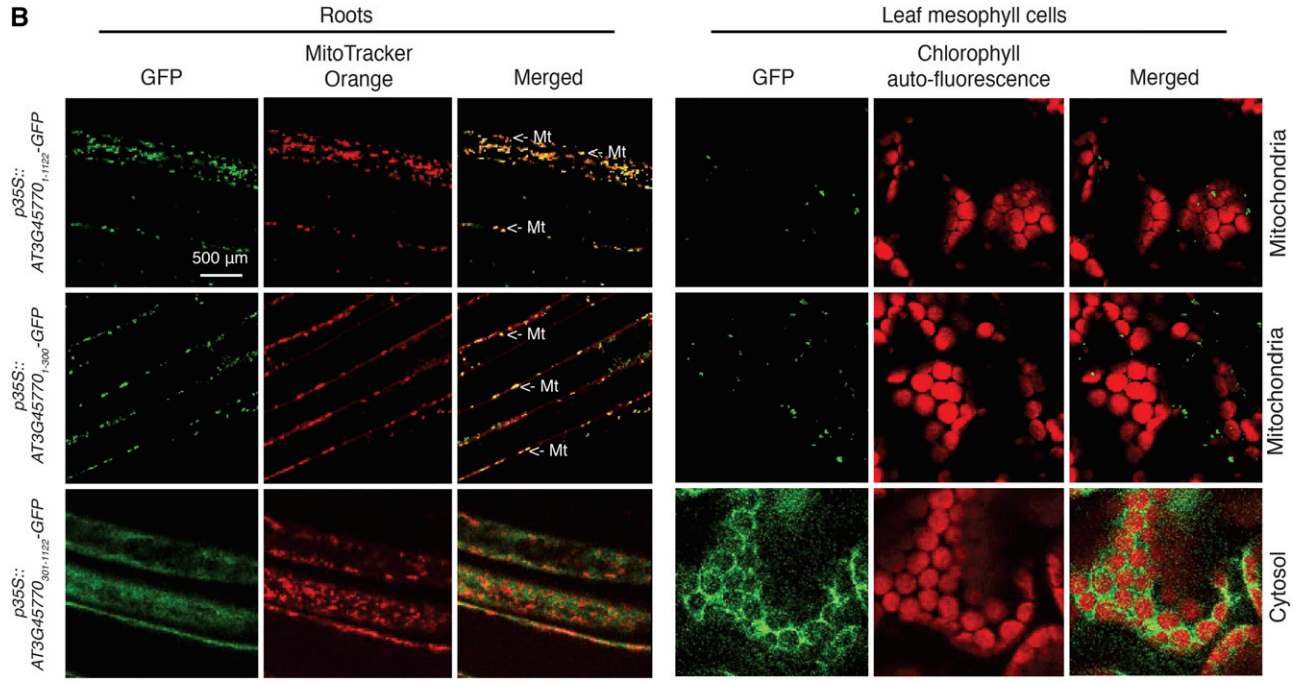

Figure 1. Continued.

strategies. In the first series of experiments, the catalytic function of the putative mtFAS component proteins was evaluated by expressing each protein in *S. cerevisiae* mutant strains that lack a functional copy of an mtFAS component and testing for genetic complementation. The expression of each candidate Arabidopsis protein was accurately targeted to yeast mitochondria, by genetically fusing the mitochondrial presequence of the yeast COQ3 protein (Hsu et al., 1996) to the N terminus of the mature Arabidopsis proteins, and their expression

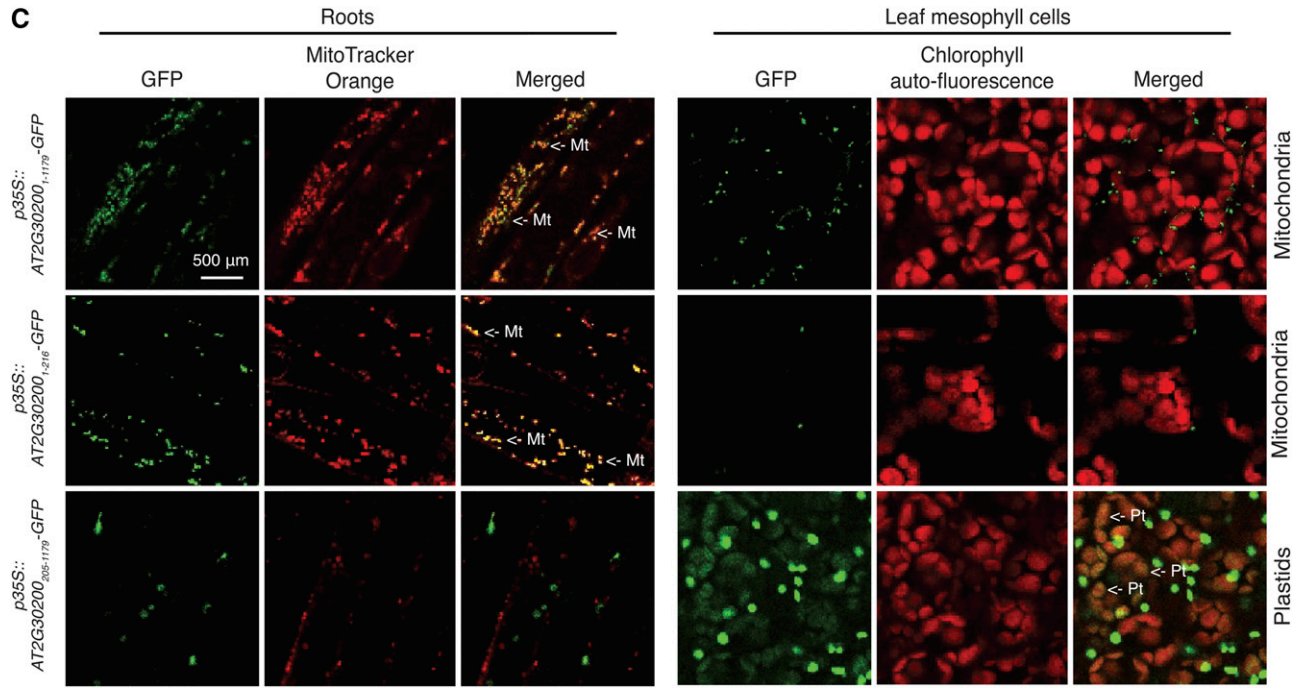

Figure 1. Continued.

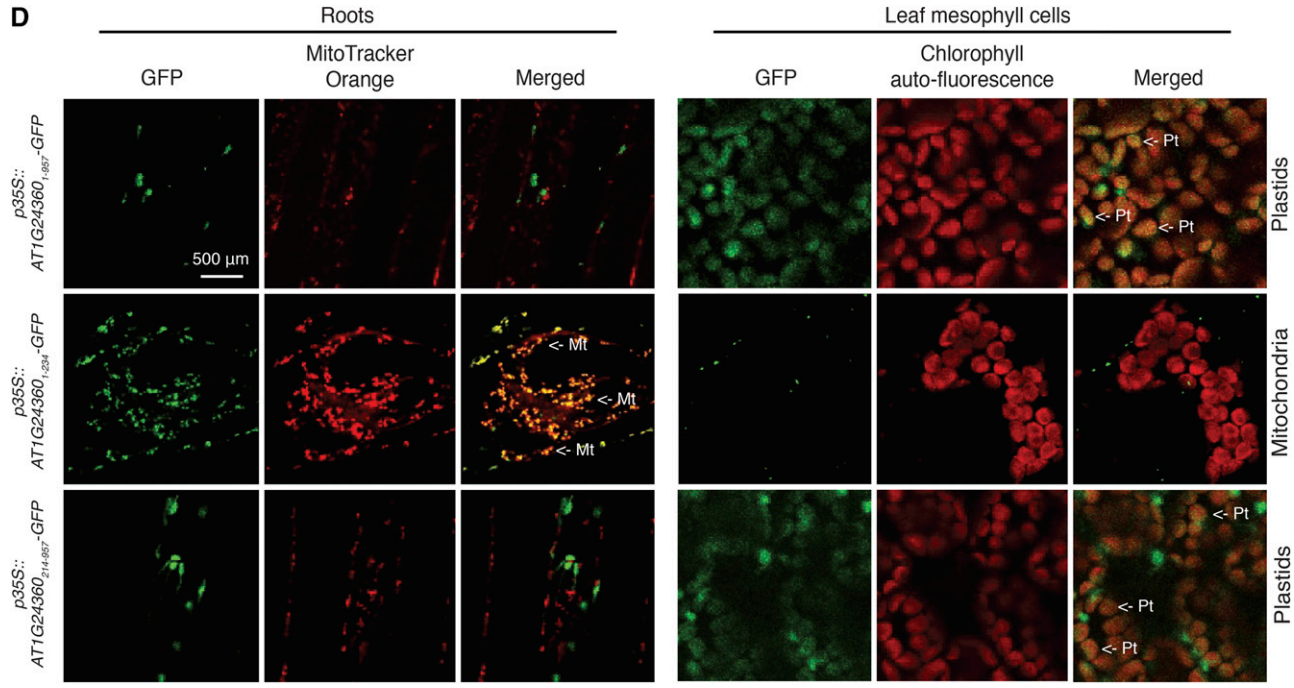

Figure 1. Continued.

in yeast was under the transcriptional control of the constitutive phosphoglycerate kinase (PGK) promoter (de Moraes et al., 1995).

The yeast mutant strains that lack mtFAS functions cannot utilize glycerol as a sole carbon source because they are deficient in respiration (Torkko et al., 2001). On media that use glycerol as the sole carbon source, the yeast mutant strains lacking individual mtFAS components (i.e. *mct1*, *oar1*, or *etr1*) showed no growth unless they expressed the mitochondrially targeted Arabidopsis proteins encoded by AT2G30200, AT1G24360, AT2G05990, or AT3G45770 (Fig. 2A). In each case, these results

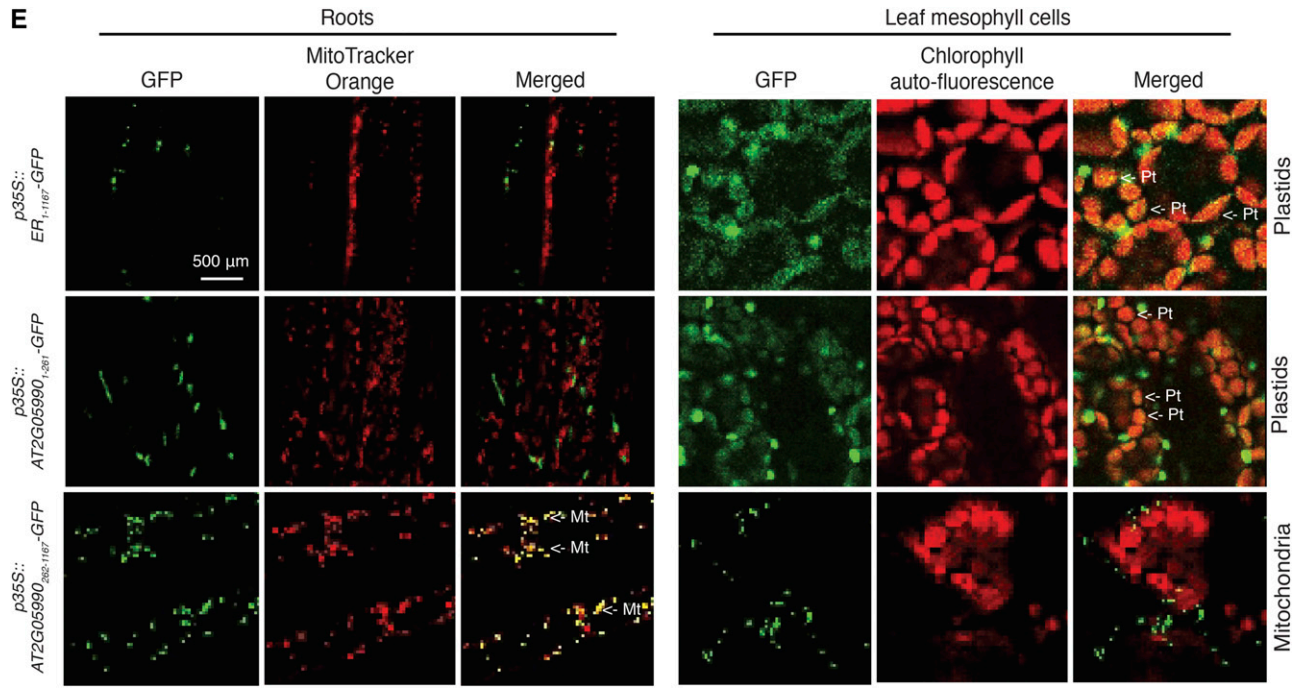

Figure 1. Continued.

mirrored the results obtained by similarly expressing the yeast MCT1, OAR, or ETR1 protein (Fig. 2A). In contrast, neither the control empty expression plasmid nor the expression plasmid carrying only the *COQ3* mitochondrial targeting element rescued the growth deficiency of these yeast strains in glycerol media (Fig. 2A).

In the case of the ER components of the mtFAS system, recombinant purified proteins encoded by AT2G05990 or AT3G45770 (expressed in *E. coli*) were also evaluated in vitro for their ability to catalyze the expected chemical reaction. Because ERs are active with both enoyl-ACP (their native substrate) and enoyl-CoA (Chen et al., 2008), in these experiments each protein was tested for the ability to reduce enoyl-CoA substrates. These assays were conducted with $\Delta 2^{trans}$-10:1-CoA and $\Delta 2^{trans}$-16:1-CoA, and activity was monitored by the decrease in A_{340} due to the coupled oxidation of the pyrimidine nucleotides (NADH or NADPH). Both AT2G05990 and AT3G45770 proteins were capable of reducing the enoyl-CoA substrates, and they exhibited comparable K_m, V_{max}, and catalytic efficiency (k_{cat}/K_m) with both tested substrates (Fig. 2B). Moreover, these assays established that AT2G05990 is an NADH-dependent reductase, and

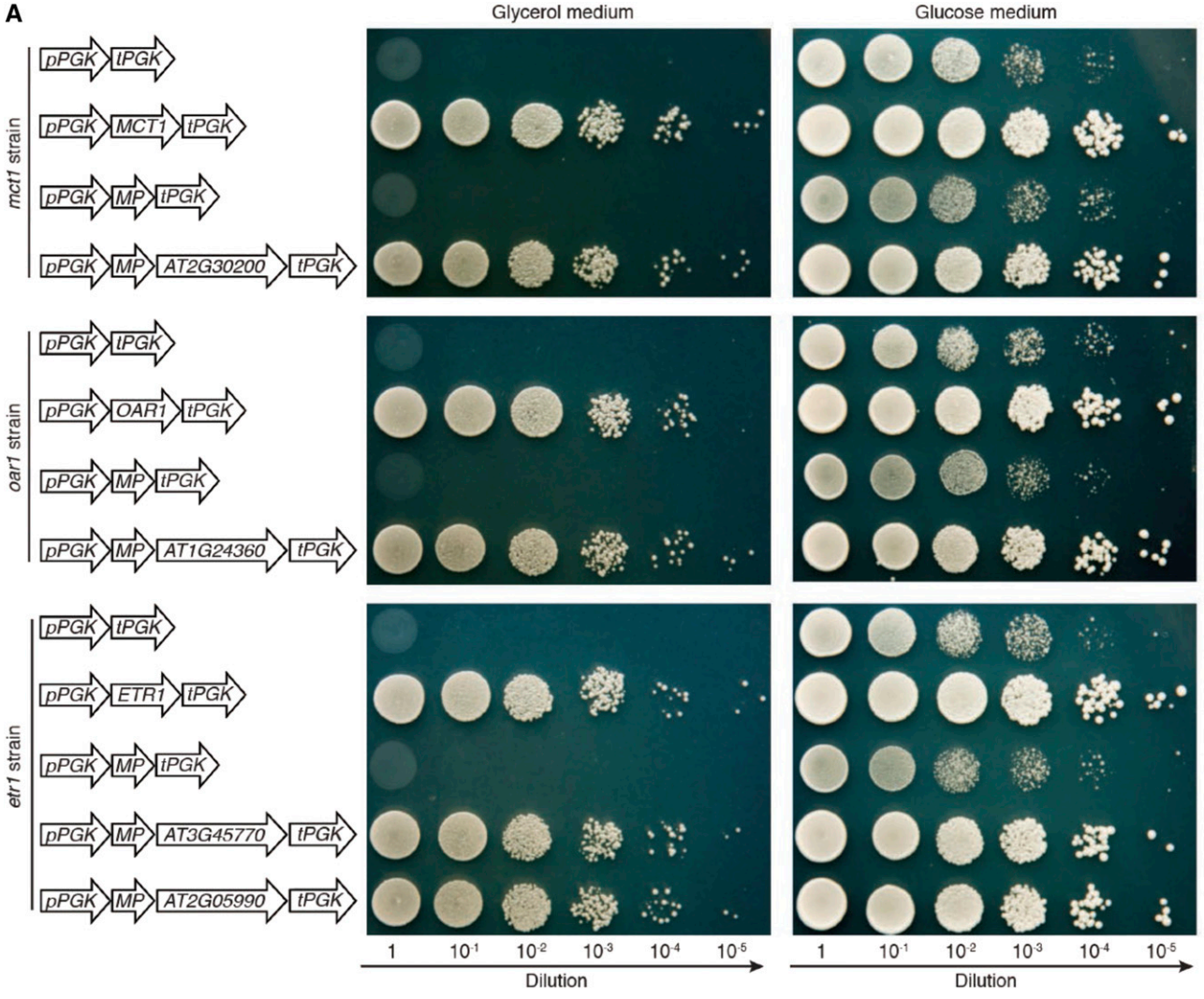

Figure 2. Genetic and biochemical characterization of mtFAS gene candidates. A, Genetic complementation of yeast mtFAS mutants (*mct1*, *oar1*, and *etr1*) by expression of Arabidopsis mtFAS candidate genes (AT2G30200, AT1G24360, AT3G45770, and AT2G05990); expression of the wild-type yeast homologs (*MCT1*, *OAR1*, and *ETR1*) served as a positive control. Gene expression was transcriptionally controlled by the PGK promoter (*pPGK*) and terminator (*tPGK*). The mitochondrial presequence of yeast COQ3 protein was fused to the N terminus of each protein to ensure mitochondrial localization. All yeast strains, carrying the indicated expression cassettes, were grown on medium containing either glycerol or Glc as the sole carbon source, and a dilution series served as the inoculum for each strain. B, In vitro characterization of the catalytic capability of purified recombinant Arabidopsis mtER and pt/mtER enzymes. Substrate concentration dependence of the enoyl reductase activity was assayed with increasing concentrations of either trans-Δ^2-10:1-CoA or trans-Δ^2-16:1-CoA as substrate. The tabulated Michaelis-Menten kinetic parameters were calculated from three to six replicates for each substrate concentration.

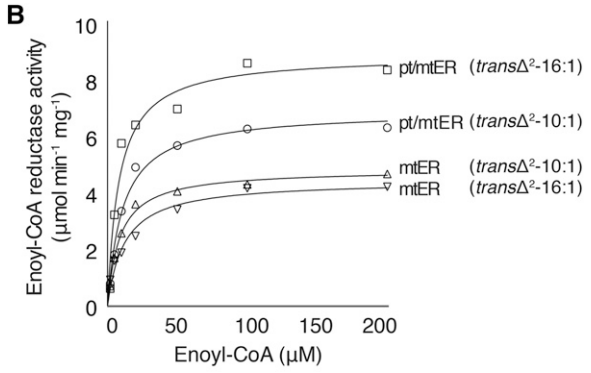

Enzyme	Enyol-CoA substrate	Km (μM)	Vmax (μmol min^{-1} mg^{-1})	kcat/Km (μM^{-1} min^{-1})
mtER	*trans*-Δ^2-10:1	8.8 ± 0.9	4.8 ± 0.1	0.87 ± 0.09
mtER	*trans*-Δ^2-16:1	12.1 ± 2.4	4.4 ± 0.2	0.58 ± 0.12
pt/mtER	*trans*-Δ^2-10:1	10.9 ± 1.6	6.8 ± 0.3	1.11 ± 0.16
pt/mtER	*trans*-Δ^2-16:1	8.3 ± 2.2	8.8 ± 0.6	1.88 ± 0.67

Figure 2. Continued.

its activity with NADPH was undetectable. In contrast, AT3G45770 is an NADPH-dependent reductase, and its activity with NADH was undetectable.

In combination, therefore, the GFP transgenic fluorescence data, the yeast genetic complementation experiments, and the biochemical characterizations of purified proteins indicated that three Arabidopsis genes (AT2G30200, AT1G24360, and AT2G05990) encode proteins that are dual targeted to plastids and mitochondria, and they have the ability to catalyze the MCAT, KR, and ER reactions, respectively. We therefore labeled these proteins as malonyl-coenzyme A:ACP transacylase (pt/mtMCAT; AT2G30200), β-ketoacyl-ACP reductase (pt/mtKR; AT1G24360), and enoyl-ACP reductase (pt/mtER; AT2G05990), indicating their dual localizations. In contrast, AT3G45770 encoded a mitochondrially localized ER enzyme, which we labeled as mtER, indicating its functionality in the sole organelle.

The in Planta Roles of pt/mtMCAT and pt/mtKR in mtFAS

The role of pt/mtMCAT (AT2G30200) and pt/mtKR (AT1G24360) as enzymatic components of the mtFAS system was further evaluated by characterizing Arabidopsis plants carrying T-DNA-tagged mutant alleles at each locus (for details, see "Materials and Methods"). As previously described (Bryant et al., 2011), mutant plants homozygous for the T-DNA allele at the AT2G30200 locus are not recoverable, as they are embryo lethal. Similarly, mutant plants homozygous for the T-DNA allele at AT1G24360 also display an embryo-lethal phenotype. This embryo lethality is associated with the fact that these two gene products are components of the ptFAS system (Bryant et al., 2011), which prior genetic studies have established as being essential; these genetic conclusions are exemplified by mutations in other ptFAS components, such as the heteromeric acetyl-CoA carboxylase (Li et al., 2011b) and 3-ketoacyl-ACP synthase I (Wu and Xue, 2010).

Therefore, we designed transgenic complementation experiments to further confirm that these dual-localized gene products are also components of the mtFAS system. Specifically, plants that were heterozygous mutants at the AT2G30200 locus (pt/mtMCAT) or the AT1G24360 locus (pt/mtKR) were transformed with transgenes that express two versions of the pt/mtMCAT or pt/mtKR proteins, respectively. One version of these transgenes expressed the ORF that encodes the full-length proteins, and as indicated by the GFP transgenic localization experiments, these full-length proteins contained both an N-terminal, mitochondrial targeting presequence and an internal plastid-targeting signal. These proteins would therefore be expected to be dual targeted to both plastids and mitochondria. The other version of these proteins expressed ORFs missing the N-terminal targeting presequence (removing the first 68 and 71 amino acids, respectively, from the full-length proteins) and thereby deleting the mitochondria-targeting information from each protein. These truncated proteins contained only the internal plastid-targeting signal and thereby would be expected to express these catalytic functions only in plastids but not in mitochondria.

Compared with the nontransgenic siblings, which failed to generate homozygous mutant plants (due to missing ptFAS function), all four recovered transgenic lines generated homozygous mutant progeny plants. At 16 d after imbibition (DAI), the transgenic plants, which expressed the full-length pt/mtMCAT or pt/mtKR proteins, were indistinguishable from wild-type plants, indicating that these transgenically expressed proteins complemented the deficiency in both mtFAS and ptFAS function.

In contrast, the transgenic plants expressing the N-terminally truncated pt/mtMCAT or pt/mtKR proteins (i.e. these proteins were predicted to be plastid localized but not targeted to mitochondria) exhibited reduced size (Fig. 3A). Most significantly, when these plants were grown in a 1% (v/v) CO_2 atmosphere, where photorespiration deficiency is suppressed, the stunted growth morphology was reversed (Fig. 3A). Further biochemical analyses of these plants established that the lipoylation status of the H-protein subunit of GDC was reduced to less than 10% of the control levels (Fig. 3B). Analogous immunoblot analyses revealed the lipoylation states of three additional lipoylated proteins, namely the E2 subunits of mitochondrial PDH and KGDH and the E2 subunit of the plastidial PDH (Supplemental Fig. S2); the E2 subunit of BCKDH was not detectable (Ewald et al., 2007).

As a consequence of the reduced lipoylation of the H-protein, Gly levels were induced by about 100-fold in these plants (Fig. 3C). Growing these transgenic mutant plants in the 1% (v/v) CO_2 atmosphere restored the accumulation of Gly to nearly control levels (Fig. 3C). Changes in the levels of other amino acids were barely detectable (Supplemental Fig. S3).

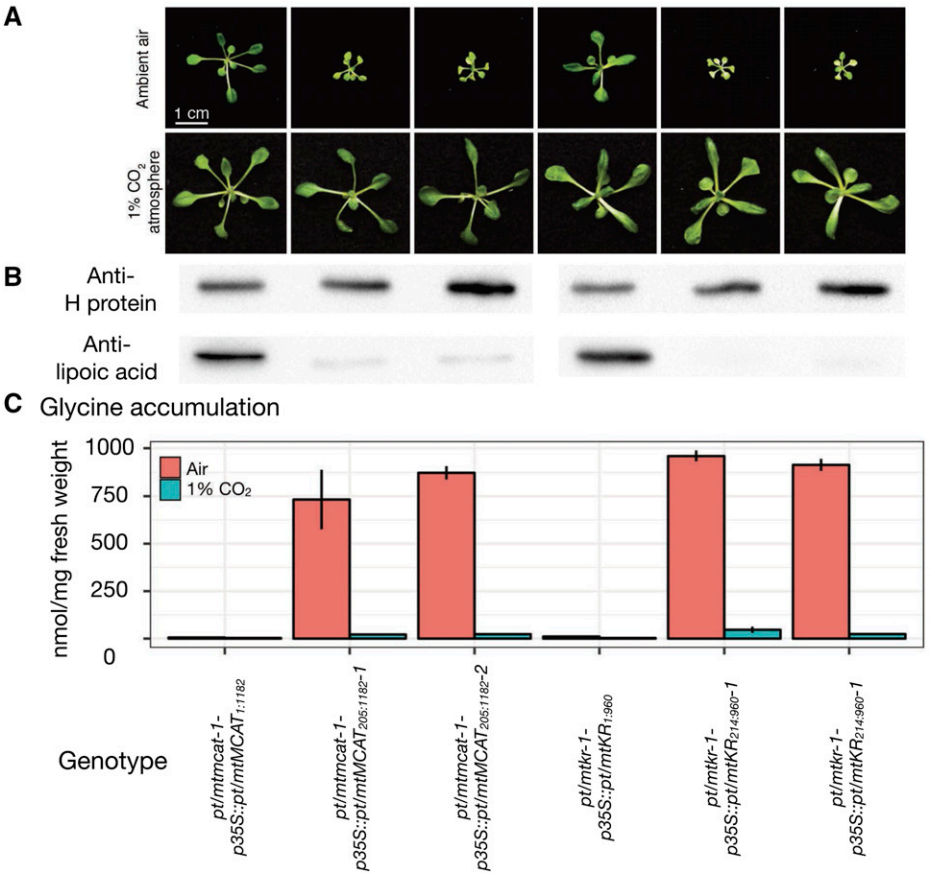

Figure 3. In vivo physiological characterization of the *pt/mtMCAT* and *pt/mtKR* genes. A, Morphological phenotypes of the *pt/mtmcat* and *pt/mtkr* mutants complemented by full-length or truncated transgenes. Plants were grown in either ambient air or in a 1% (v/v) CO_2 atmosphere. B, Western-blot analysis of the H subunit of GDC detected with either anti-H-protein antibodies or anti-lipoic acid antibodies, detecting the lipoylation status of the H-protein. C, Gly accumulation. Plants of the indicated genotypes were grown in either ambient air or in a 1% CO_2 atmosphere.

The reduced lipoylation of the H-protein of GDC is an attribute previously characterized with mutations in other mtFAS components, such as mtKAS (Ewald et al., 2007), mtHD (Guan et al., 2017), mtPPT (Guan et al., 2015), mtMCS (Guan and Nikolau, 2016), and mtACP (Fu et al., 2020). These latter mutants exhibit a growth stunting that is reversible when plants are grown in an elevated CO_2 atmosphere. Such characteristics have been attributed to the fact that mtFAS generates the lipoic acid cofactor for GDC, and this deficiency blocks photorespiration, leading to the growth deficiency, and hyperaccumulation of Gly, traits that are all reversed when mtFAS mutant plants are grown in an elevated CO_2 atmosphere that suppresses photorespiration (Guan et al., 2017). Collectively, therefore, these findings demonstrate that the MCAT and KR catalytic functions of the mtFAS and ptFAS systems are genetically encoded by two respective genes that each encode dual-localized proteins, pt/mtMCAT and pt/mtKR.

Two ER Isozymes for mtFAS

Two genetic loci appear to encode proteins that catalyze the enoyl-ACP reduction reaction of mtFAS: the AT2G05990 locus, which encodes an NADH-dependent reductase, and the AT3G45770 locus, which encodes an NADPH-dependent reductase. The former protein was dual targeted (i.e. pt/mtER), and the latter was targeted to mitochondria (i.e. mtER). We genetically dissected the roles of these two ER genes by characterizing three mutant lines: (1) two T-DNA-tagged mutant alleles at the mtER locus (*mter-1* and *mter-2*), both of which eliminated the expression of mtER; (2) RNA interference (RNAi) knockdown lines of the *pt/mtER* locus (*pt/mter-rnai-1* and *pt/mter -rnai-2*), which reduced the expression of pt/mtER to ~2% of wild-type levels; and (3) double mutant lines (i.e. *mter-1-pt/mter-rnai-1* and *mter-1-pt/mter-rnai-2*), which eliminated the expression of mtER and reduced the expression of pt/mtER to ~2% of wild-type levels (Fig. 4).

As indicated by the exemplary data gathered from plants at 16 DAI, plants homozygous for the mutant *mtER* alleles were morphologically and metabolically (i.e. amino acids, fatty acids, and lipids) indistinguishable from wild-type plants (Supplemental Table S1). In contrast, the aerial organs of the *pt/mter-rnai* mutant and *mter-1-pt/mter-rnai* double mutant lines were considerably reduced in size (Fig. 4A). This growth phenotype was equally expressed independent of whether these plants were grown in ambient air or a 1% (v/v) CO_2 atmosphere (Fig. 4A); the expectation being that in the latter conditions any potential mtFAS-associated photorespiration phenotype would be suppressed (Ewald et al., 2007). Therefore, these observations suggest that these mutations do not affect mtFAS, and they are consistent with prior characterization of an ethyl

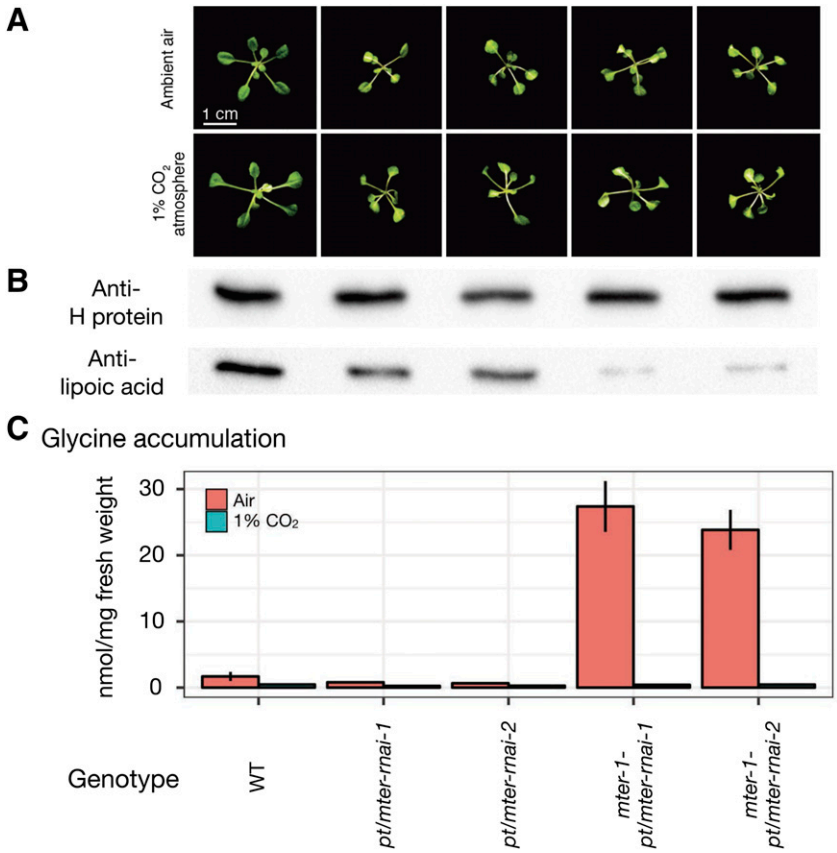

Figure 4. Physiological characterization of the *pt/mtER* and *mtER* genes. A, Morphological phenotypes of single or double mutants of the *pt/mtER* and *mtER* genes. Plants were grown in either ambient air or in a 1% (v/v) CO_2 atmosphere. B, Western-blot analysis of the H subunit of GDC detected with anti-H-protein antibodies, and the lipoylation status of the H-protein detected with anti-lipoic acid antibodies. Plants were grown in a 1% (v/v) CO_2 atmosphere. C, Gly accumulation. Plants of the indicated genotypes were grown in either ambient air or in a 1% (v/v) CO_2 atmosphere. WT, Wild type.

methanesulfonate-generated *pt/mter* mutant (Mou et al., 2000; Wu et al., 2015) that identified this gene product as a component of the ptFAS system.

In contrast, biochemical analyses that evaluated the metabolic status of these mutant plants indicated that both *mtER* and *pt/mtER* contribute to mtFAS. The evidence that supports this conclusion includes the following: (1) immunoblot analysis that indicated the lipoylation states of GDC in *mter* and *pt/mter-rnai* single mutants were reduced to 60% to 80% of the wild-type levels, and this protein was even further underlipoylated to about 10% of the wild-type level in the double mutant plants (Fig. 4B); (2) accompanied by the reduction in lipoylation status of the H-protein, Gly accumulation was increased by about 15-fold in these double mutant lines; and (3) this latter attribute was completely reversed when these double mutant plants were grown in the 1% (v/v) CO_2 atmosphere, which suppresses photorespiration (Fig. 4C). Other changes in amino acid levels were detected in these double mutants (Supplemental Table S1). Collectively, therefore, we conclude that the mtFAS system appears to be redundantly enabled by two ERs, pt/mtER (AT2G05990) and mtER (AT3G45770).

DISCUSSION

As a consequence of the evolutionary origin of mitochondria and plastids as eubacterial symbionts in eukaryotic cells (Gray, 2004), plant cells have maintained two type II FAS systems that are located in these organelles. Whereas the genetic and enzymatic components of the ptFAS system have received considerable attention (Ohlrogge and Jaworski, 1997), the analogous components of the mtFAS system are only just being characterized (Guan et al., 2015, 2017; Guan and Nikolau, 2016; Fu et al., 2020). This complexity associated with organelle specificity of the FAS systems is further complicated by the genetic redundancy that has been revealed by the genomic-based bioinformatic analysis of plant genomes, as revealed by Li-Beisson et al. (2013). This study completes the identification and characterization of the core catalytic components of the mtFAS system. These characterizations unexpectedly find that some of these components are shared between the ptFAS and mtFAS systems, which was not predictable based solely on bioinformatic analysis of genomic data (Beisson et al., 2003).

Dual-Localized MCAT, KR, and ER Components of mtFAS

The plant mtFAS system is a pathway that contributes acyl substrates required for a series of essential metabolic processes, including photorespiration and biosynthesis of lipid A-like molecules (Guan et al., 2017). To date, four enzymatic components of the mtFAS system have been experimentally characterized: mtKAS (Olsen et al., 2004; Yasuno et al., 2004; Ewald

et al., 2007), mtHD (Guan et al., 2017), mtPPT (Guan et al., 2015), and mtMCS (Guan and Nikolau, 2016). In this study, we identified the additional three components that are required to complete the mtFAS cycle. These three components (pt/mtMCAT, pt/mtKR, and pt/mtER) localized to both plastids and mitochondria, referred to as dual targeted, and thus they contribute to both mtFAS and ptFAS capabilities. In addition, the mitochondrial ER reaction appears to be catalyzed by redundant enzymes, an NADPH-dependent mtER and a dual-targeted NADH-dependent pt/mtER. The pt/mtER and mtER belong to two distinct families of enzymes; pt/mtER belongs to the short-chain dehydrogenase/reductase family, whereas mtER belongs to the medium-chain dehydrogenase/reductase family (Hiltunen et al., 2010). Despite the distinct preference for different reducing cofactors (NADH versus NADPH), both pt/mtER and mtER display a similar chain length preference for the 2-enoyl substrates, being able to almost equally utilize both medium-chain (10 carbon atoms) and long-chain (16 carbon atoms) substrates. This latter finding is consistent with the ability of the plant mtFAS system to not only generate octanoic acid for lipoic acid biosynthesis but also longer chain fatty acids that are used in the assembly of lipid A-like molecules (Guan et al., 2017).

The dual-localized mtFAS components (i.e. pt/mtMCAT and pt/mtKR) had previously been characterized as components of the ptFAS system (Mou et al., 2000; Wu and Xue, 2010; Bryant et al., 2011), and these characterizations had established the essentiality of these components and the ptFAS system during embryogenesis. Thus, deducing that these are also components of the mtFAS system required a combination of reverse genetic and transgenic strategies. Specifically, we generated plants that were deficient in mitochondrial MCAT or KR functions but normally expressed plastid-localized MCAT or KR functions. This could be achieved by the fact that for these two proteins, the plastid-targeting information is encompassed within the mature protein sequence, whereas the mitochondria-targeting information is encompassed in the N-terminal signal-peptide extension sequence. Thus, the transgenically expressed, N-terminally truncated MCAT or KR proteins were singly targeted to plastids rather than to both the plastids and mitochondria. Therefore, these transgenically plastid-only retargeted MCAT or KR alleles rescued the embryo-lethal phenotypes associated with the deficiency in ptFAS, but the recovered transgenic plants displayed phenotypes that are typical of plants lacking mtFAS functionality. These phenotypes include reduced H-protein lipoylation, elevated Gly accumulation, and reduced growth; the latter two attributes being reversed by growing plants in a CO_2-enriched atmosphere. Because these biochemical traits are commonly expressed with other mutations that affect mtFAS, these findings are consistent with the role that these two gene products have in providing the MCAT or KR enzymatic functions of the mtFAS system, respectively.

The characterization of the mitochondrial ER component was more complex because two loci can provide this functionality, a dual-localized pt/mtER (AT2G05990) and a singly targeted mtER (AT3G45770). Plants deficient in mitochondrial ER function were generated by combining mutants that affect both loci, using a combination of T-DNA-tagged null alleles at AT3G45770 and RNAi knockdown alleles of AT2G05990. These plants exhibited traits that are typical of a deficiency in mtFAS: namely, depleted lipoylation of the H-protein, hyperaccumulation of Gly, and miniature aerial organs. All these traits appear when these plants are grown in ambient air, and Gly hyperaccumulation is reversed when they are grown in an elevated-CO_2 atmosphere.

Dual Localization of Proteins to Plastids and Mitochondria

Proteomic analyses of isolated organelles have indicated that a number of proteins (greater than 100) generated from a single gene locus may be dual targeted to both mitochondria and plastids (Carrie et al., 2009b). Although this conclusion is based on experimental outcomes that are fraught with technical challenges associated with the ability to purify distinct organelle preparations (van Wijk and Baginsky, 2011; Rao et al., 2017), the use of fluorescently tagged proteins substantiates the occurrence of this phenomenon, although even these experiments need to be carefully considered (Sharma et al., 2018a, 2018b). In this study, we presented GFP localization studies that substantiate the global proteomics evidence concerning dual plastid-mitochondrial localization conclusions. Additional molecular genetic studies used transgenic constructs to retarget the dual-localized proteins to either plastids or mitochondria. These experiments confirmed that the plastid-retargeted constructs only affected the ptFAS-associated outcomes and the mitochondria-retargeted constructs only affected the mtFAS-associated outcomes.

An obvious evolutionary advantage of such dual localization of products from a single gene locus would be the apparent energy and resource economy of maintaining only one gene for both organelles instead of a gene for each organelle. However, from an evolutionary point of view, concentrating two functions in a single gene locus is unusual, as the more common tendency is for neospecialization following gene duplications (Carrie and Small, 2013). In addition, there are clear disadvantages for dual-targeted proteins. For example, the protein may not function optimally in both organelles, in terms of pH optima, concentration of substrates and cofactors, and protein-protein interactions. Moreover, a single crucial mutation could lead to the loss of this function in both organelles.

Insights may be provided by considering the functions of the proteins that are known to be dual targeted. Dual-targeted proteins appear to be enriched in a few specific functional groups (Carrie and Small, 2013), such as DNA replication, tRNA biogenesis, protein translation, and metabolic processes (e.g. fatty acid

biosynthesis, as demonstrated in this study). This potential bias may reflect mechanistic constraints on dual targeting and selection pressure that could favor dual targeting over evolutionary time scales.

Mechanistically, for dual targeting between mitochondria and plastids, the targeted protein has to be recognized by the import machinery of both organelles (Carrie et al., 2009a). Evolutionarily, the protein-import machineries in these organelles arose independently, are nonhomologous, and therefore would normally be expected to recognize different targeting signals (Schleiff and Becker, 2011). Indeed, in the case of pt/mtMCAT, pt/mtKR, and pt/mtER, these proteins appear to utilize bipartite targeting signals, an N-terminal signal unique for one organelle and an internal signal that specifies import to the other organelle. Deletion of the N-terminal signal of pt/mtMCAT and pt/mtKR abolishes import into mitochondria and enhances import into plastids, whereas the contrary was observed for pt/mtER. Similar situations have been reported with many other such dual-targeted proteins (e.g. the amino acyl-tRNA synthetases AspRS, LysRS, and ProRS [Berglund et al., 2009a, 2009b], the mitochondrial carrier protein BT1 [Bahaji et al., 2011], and phosphatidyl glycerophosphate synthase1 [Babiychuk et al., 2003]); deletion of their N-terminal targeting sequences only affects localization to one of these two organelles. In the case of the mtER isozyme, deletion of the N-terminal targeting sequence resulted in the cytosolic localization of the protein, indicating the presence of an additional signal that is needed for dual localization.

Dual localization of pt/mtMCAT, pt/mtKR, and pt/mtER, a trait acquired during the coevolution of plastids and mitochondria, suggests that further investigations of protein-sorting mechanisms and reevaluation of organelle proteomes may be useful to reveal how generalizable this phenomenon is in plant cells. Moreover, the general persistence of such genetic and biochemical redundancy in plant metabolism may indicate evolutionary biological advantages to the generation of such complexity in metabolism, a characteristic that was initially surmised from the study of specialized metabolism (Pichersky and Lewinsohn, 2011).

MATERIALS AND METHODS

Yeast Strains and Genetic Complementation

The yeast (*Saccharomyces cerevisiae*) strain deficient in the *MCT1*, *OAR1*, and *ETR1* genes (YBR026C; BY4741 background; and MATa) was obtained from Thermo Scientific. The yeast *MCT1* (primers M1 and M2; see Supplemental Table S2 for primer sequences), *OAR1* (primers M3 and M4), and *ETR1* (primers M5 and M6) genes of wild-type BY4741 strain were cloned into YEp351 vector (PGK promoter-driven gene expression; de Moraes et al., 1995). Arabidopsis (*Arabidopsis thaliana*) *pt/mtMCAT* (AT2G30200; primers M7and M8), *pt/mtKR* (AT1G24360; primers M9 and M10), *pt/mtER* (AT2G05990; primers M11 and M12), and *mtER* (AT3G45770; primers M13 and M14) genes of the Columbia-0 (Col-0) strain were cloned into YEp351M (Guan et al., 2017; 5′ plant targeting signals were replaced by the yeast *COQ3* mitochondrial presequence coding sequence). Complementation tests were performed as previously described (Torkko et al., 2001).

Protein Overexpression and in Vitro Kinetic Assays

The *mt/ptER* (primers M15 and M16) and *mtER* (primers M17 and M18) genes were cloned into pBE522 vector (Zhu et al., 2011). These constructs express recombinant proteins with a His tag located at the N terminus. Recombinant proteins were expressed in the *Escherichia coli* BL21* strain (Invitrogen) and further purified using Probond Nickel-Chelating Resin (Invitrogen). The kinetic constants of mt/ptER and mtER were determined spectrophotometrically as previously described (Chen et al., 2008) with modification. Specifically, the enoyl-CoA substrates (i.e. trans-Δ^2-10:1 and trans-Δ^2-16:1) were synthesized as previously described (Guan et al., 2017). Concentrations of three ingredients were optimized (i.e. 30 mM potassium phosphate [pH 7.8], 2 to 200 μM enoyl-CoA, 300 μM NADPH or NADH, and 3 μg mL^{-1} recombinant proteins). The consumption of NADPH or NADH at 340 nm (for 0, 5, 10, 15, and 20 min at 22°C) was measured to monitor the enoyl-CoA reduction reaction. Kinetic values for mt/ptER and mtER were calculated using Prism version 5.0 (GraphPad Software).

Plant Strains and Genetic Transformations

The Arabidopsis genetic strains used in this study included *mcat-1* (Landsberg *erecta* background; GT_5_100190), *kr-1* (Col-3 background; SAIL_165_A11), *mter-1* (Col-0 background; SALK_056770), and *mter-2* (Col-0 background; SALK_085297), which were obtained from the Arabidopsis Biological Resource Center (http://abrc.osu.edu).

In the GFP transgene experiments, PCR inserts were obtained using the following primer pairs: *pt/mtMCAT*$_{1\text{-}1179}$ (primers M19 and M20), *pt/mtMCAT*$_{1\text{-}216}$ (primers M19 and M21), *pt/mtMCAT*$_{205\text{-}1179}$ (primers M22 and M20), *pt/mtKR*$_{1\text{-}957}$ (primers M23 and M24), *pt/mtKR*$_{1\text{-}234}$ (primers M23 and M25), *pt/mtKR*$_{214\text{-}957}$ (primers M26 and M24), *pt/mtER*$_{1\text{-}1167}$ (primers M27 and M28), *pt/mtER*$_{1\text{-}261}$ (primers M27 and M29), *pt/mtER*$_{262\text{-}1167}$ (primers M30 and M28), *mtER*$_{1\text{-}1122}$ (primers M31 and M32), *mtER*$_{1\text{-}300}$ (primers M31 and M33), *mtER*$_{301\text{-}1122}$ (primers M34 and M32), and *UGP3*$_{1\text{-}600}$ (primers M35 and M36). PCR inserts were cloned into pENTR/D-TOPO vector (Invitrogen) and subcloned into pEarleyGate103 (Earley et al., 2006) using Gateway LR Clonase II Enzyme Mix (Invitrogen).

In the complementation transgene experiment, *pt/mtMCAT*$_{1\text{-}1182}$ (primers M19 and M37), *pt/mtMCAT*$_{205\text{-}1182}$ (primers M22 and M37), *pt/mtKR*$_{1\text{-}960}$ (primers M23 and M38), and *pt/mtKR*$_{214\text{-}960}$ (primers M26 and M38) were cloned into pENTR/D-TOPO vector and subcloned into pEarleyGate100 (Earley et al., 2006). Destination vectors were used to transform the Arabidopsis heterozygous mutant plants deficient in *pt/mtMCAT* and *pt/mtKR*.

In the RNAi experiment, *pt/mtER*$_{202\text{-}380}$ (primers M39 and M40) was cloned into pENTR/D-TOPO and subcloned into pB7GWIWG2(II) (Karimi et al., 2002). Destination vectors were used to transform the Arabidopsis wild-type plants or *mter-1* mutant plants as previously described.

Plant seedlings were grown on Murashige and Skoog agar medium at 22°C under continuous illumination (photosynthetic photon flux density of 100 μmol m^{-2} s^{-1}) as previously described (Jin et al., 2012). The atmospheric CO_2 condition was maintained in the ambient level or the 1% (v/v) CO_2 level (in a growth chamber).

Immunoblot Analyses

Total protein was extracted from 200 mg of fresh aerial organs of plants at 16 DAI as described previously (Che et al., 2002). Immunoblot analysis was carried out with anti-lipoic acid antibodies (EMD Millipore) or with anti-H-protein antibodies (a gift from Dr. David Oliver at Iowa State University) on 50 μg of total protein as described previously (Ewald et al., 2007; Guan et al., 2015).

Metabolomic Analyses

Metabolites (three to six replicates) were extracted from 50 mg of fresh aerial organs of plants (grown in a completely randomized design) at 16 DAI and analyzed using multiple analytical platforms: Agilent 7890 GC-MS system for fatty acids (Lu et al., 2008); Agilent 1200 HPLC system equipped with a fluorescence detector for amino acids (Guan et al., 2015); and Waters Xevo G2 Q-TOF MS equipped with Waters ACQUITY UPLC system for glycerolipids and chlorophylls (Okazaki et al., 2015). Log_2 ratio and SE were calculated as described previously (Quanbeck et al., 2012).

Accession Numbers

Accession numbers are as follows: AT2G30200, mt/ptMCAT; AT1G24360, mt/ptKR; AT3G45770, mtER; and AT2G05990, pt/mtER.

Supplemental Data

The following supplemental materials are available.

Supplemental Figure S1. Arabidopsis gene candidates.

Supplemental Figure S2. Western-blot analysis of the lipoylation status of the indicated lipoylated proteins detected with anti-lipoic acid antibodies.

Supplemental Figure S3. Amino acid accumulation in *pt/mtmcat* and *pt/mtkr* mutants.

Supplemental Table S1. Metabolic profiling data.

Supplemental Table S2. Nucleic acid sequences of DNA primers used in this study.

ACKNOWLEDGMENTS

We thank Kouji Takano (RIKEN Center for Sustainable Resource Science) for technical assistance in obtaining the lipidome data; Drs. Lloyd Sumner (University of Missouri) and Richard Dixon (University of North Texas) for helpful discussions; and the W.M. Keck Metabolomics Research Laboratory and the Confocal Microscopy Facility (Iowa State University) for providing access to instrumentation in the metabolomic analyses and subcellular localization studies, respectively.

Received January 3, 2020; accepted March 23, 2020; published April 3, 2020.

LITERATURE CITED

Babiychuk E, Müller F, Eubel H, Braun HP, Frentzen M, Kushnir S (2003) Arabidopsis phosphatidylglycerophosphate synthase 1 is essential for chloroplast differentiation, but is dispensable for mitochondrial function. Plant J **33:** 899–909

Bahaji A, Ovecka M, Bárány I, Risueño MC, Muñoz FJ, Baroja-Fernández E, Montero M, Li J, Hidalgo M, Sesma MT, et al (2011) Dual targeting to mitochondria and plastids of AtBT1 and ZmBT1, two members of the mitochondrial carrier family. Plant Cell Physiol **52:** 597–609

Beisson F, Koo AJ, Ruuska S, Schwender J, Pollard M, Thelen JJ, Paddock T, Salas JJ, Savage L, Milcamps A, et al (2003) Arabidopsis genes involved in acyl lipid metabolism: A 2003 census of the candidates, a study of the distribution of expressed sequence tags in organs, and a web-based database. Plant Physiol **132:** 681–697

Berglund AK, Pujol C, Duchene AM, Glaser E (2009a) Defining the determinants for dual targeting of amino acyl-tRNA synthetases to mitochondria and chloroplasts. J Mol Biol **393:** 803–814

Berglund AK, Spånning E, Biverståhl H, Maddalo G, Tellgren-Roth C, Mäler L, Glaser E (2009b) Dual targeting to mitochondria and chloroplasts: Characterization of Thr-tRNA synthetase targeting peptide. Mol Plant **2:** 1298–1309

Bryant N, Lloyd J, Sweeney C, Myouga F, Meinke D (2011) Identification of nuclear genes encoding chloroplast-localized proteins required for embryo development in Arabidopsis. Plant Physiol **155:** 1678–1689

Carrie C, Giraud E, Whelan J (2009a) Protein transport in organelles: Dual targeting of proteins to mitochondria and chloroplasts. FEBS J **276:** 1187–1195

Carrie C, Kühn K, Murcha MW, Duncan O, Small ID, O'Toole N, Whelan J (2009b) Approaches to defining dual-targeted proteins in Arabidopsis. Plant J **57:** 1128–1139

Carrie C, Small I (2013) A reevaluation of dual-targeting of proteins to mitochondria and chloroplasts. Biochim Biophys Acta **1833:** 253–259

Che P, Wurtele ES, Nikolau BJ (2002) Metabolic and environmental regulation of 3-methylcrotonyl-coenzyme A carboxylase expression in Arabidopsis. Plant Physiol **129:** 625–637

Chen ZJ, Pudas R, Sharma S, Smart OS, Juffer AH, Hiltunen JK, Wierenga RK, Haapalainen AM (2008) Structural enzymological studies of 2-enoyl thioester reductase of the human mitochondrial FAS II pathway: New insights into its substrate recognition properties. J Mol Biol **379:** 830–844

de Moraes LM, Astolfi-Filho S, Oliver SG (1995) Development of yeast strains for the efficient utilisation of starch: Evaluation of constructs that express alpha-amylase and glucoamylase separately or as bifunctional fusion proteins. Appl Microbiol Biotechnol **43:** 1067–1076

Earley KW, Haag JR, Pontes O, Opper K, Juehne T, Song K, Pikaard CS (2006) Gateway-compatible vectors for plant functional genomics and proteomics. Plant J **45:** 616–629

Ewald R, Kolukisaoglu U, Bauwe U, Mikkat S, Bauwe H (2007) Mitochondrial protein lipoylation does not exclusively depend on the mtKAS pathway of de novo fatty acid synthesis in Arabidopsis. Plant Physiol **145:** 41–48

Frentzen M, Griebau R (1994) Biosynthesis of cardiolipin in plant mitochondria. Plant Physiol **106:** 1527–1532

Fu X, Guan X, Garlock R, Nikolau BJ (2020) Mitochondrial fatty acid synthase utilizes multiple acyl carrier protein isoforms. Plant Physiol **183:** 547–557

Gray MW (2004) The evolutionary origins of plant organelles. In H Daniell, and C Chase, eds, Molecular Biology and Biotechnology of Plant Organelles: Chloroplasts and Mitochondria. Springer, Dordrecht, The Netherlands, pp 15–36

Greene JG, Greenamyre JT (1995) Characterization of the excitotoxic potential of the reversible succinate dehydrogenase inhibitor malonate. J Neurochem **64:** 430–436

Griebau R, Frentzen M (1994) Biosynthesis of phosphatidylglycerol in isolated mitochondria of etiolated mung bean (*Vigna radiata* L.) seedlings. Plant Physiol **105:** 1269–1274

Guan X, Chen H, Abramson A, Man H, Wu J, Yu O, Nikolau BJ (2015) A phosphopantetheinyl transferase that is essential for mitochondrial fatty acid biosynthesis. Plant J **84:** 718–732

Guan X, Nikolau BJ (2016) AAE13 encodes a dual-localized malonyl-CoA synthetase that is crucial for mitochondrial fatty acid biosynthesis. Plant J **85:** 581–593

Guan X, Okazaki Y, Lithio A, Li L, Zhao X, Jin H, Nettleton D, Saito K, Nikolau BJ (2017) Discovery and characterization of the 3-hydroxyacyl-ACP dehydratase component of the plant mitochondrial fatty acid synthase system. Plant Physiol **173:** 2010–2028

Hiltunen JK, Chen Z, Haapalainen AM, Wierenga RK, Kastaniotis AJ (2010) Mitochondrial fatty acid synthesis: An adopted set of enzymes making a pathway of major importance for the cellular metabolism. Prog Lipid Res **49:** 27–45

Hsu AY, Poon WW, Shepherd JA, Myles DC, Clarke CF (1996) Complementation of coq3 mutant yeast by mitochondrial targeting of the Escherichia coli UbiG polypeptide: Evidence that UbiG catalyzes both O-methylation steps in ubiquinone biosynthesis. Biochemistry **35:** 9797–9806

Jin H, Song Z, Nikolau BJ (2012) Reverse genetic characterization of two paralogous acetoacetyl CoA thiolase genes in Arabidopsis reveals their importance in plant growth and development. Plant J **70:** 1015–1032

Karimi M, Inzé D, Depicker A (2002) GATEWAY vectors for *Agrobacterium*-mediated plant transformation. Trends Plant Sci **7:** 193–195

Li C, Guan Z, Liu D, Raetz CR (2011a) Pathway for lipid A biosynthesis in *Arabidopsis thaliana* resembling that of Escherichia coli. Proc Natl Acad Sci USA **108:** 11387–11392

Li X, Ilarslan H, Brachova L, Qian HR, Li L, Che P, Wurtele ES, Nikolau BJ (2011b) Reverse-genetic analysis of the two biotin-containing subunit genes of the heteromeric acetyl-coenzyme A carboxylase in Arabidopsis indicates a unidirectional functional redundancy. Plant Physiol **155:** 293–314

Li-Beisson Y, Shorrosh B, Beisson F, Andersson MX, Arondel V, Bates PD, Baud S, Bird D, Debono A, Durrett TP, et al (2010) Acyl-lipid metabolism. The Arabidopsis Book **8:** e0133

Li-Beisson Y, Shorrosh B, Beisson F, Andersson MX, Arondel V, Bates PD, Baud S, Bird D, Debono A, Durrett TP, et al (2013) Acyl-lipid metabolism. The Arabidopsis Book **11:** e0161

Lu Y, Savage LJ, Ajjawi I, Imre KM, Yoder DW, Benning C, Dellapenna D, Ohlrogge JB, Osteryoung KW, Weber AP, et al (2008) New connections across pathways and cellular processes: Industrialized mutant screening reveals novel associations between diverse phenotypes in Arabidopsis. Plant Physiol **146:** 1482–1500

Mou Z, He Y, Dai Y, Liu X, Li J (2000) Deficiency in fatty acid synthase leads to premature cell death and dramatic alterations in plant morphology. Plant Cell **12:** 405–418

Ohlrogge JB, Jaworski JG (1997) Regulation of fatty acid synthesis. Annu Rev Plant Physiol Plant Mol Biol **48:** 109–136

Okazaki Y, Nishizawa T, Takano K, Ohnishi M, Mimura T, Saito K (2015) Induced accumulation of glucuronosyldiacylglycerol in tomato and soybean under phosphorus deprivation. Physiol Plant **155:** 33–42

Okazaki Y, Shimojima M, Sawada Y, Toyooka K, Narisawa T, Mochida K, Tanaka H, Matsuda F, Hirai A, Hirai MY, et al (2009) A chloroplastic UDP-glucose pyrophosphorylase from Arabidopsis is the committed enzyme for the first step of sulfolipid biosynthesis. Plant Cell **21:** 892–909

Olsen JG, Rasmussen AV, von Wettstein-Knowles P, Henriksen A (2004) Structure of the mitochondrial beta-ketoacyl-[acyl carrier protein] synthase from Arabidopsis and its role in fatty acid synthesis. FEBS Lett **577:** 170–174

Pichersky E, Lewinsohn E (2011) Convergent evolution in plant specialized metabolism. Annu Rev Plant Biol **62:** 549–566

Quanbeck SM, Brachova L, Campbell AA, Guan X, Perera A, He K, Rhee SY, Bais P, Dickerson JA, Dixon P, et al (2012) Metabolomics as a hypothesis-generating functional genomics tool for the annotation of Arabidopsis thaliana genes of "unknown function.". Front Plant Sci **3:** 15

Quastel JH, Wooldridge WR (1928) Some properties of the dehydrogenating enzymes of bacteria. Biochem J **22:** 689–702

Rao RS, Salvato F, Thal B, Eubel H, Thelen JJ, Møller IM (2017) The proteome of higher plant mitochondria. Mitochondrion **33:** 22–37

Schleiff E, Becker T (2011) Common ground for protein translocation: Access control for mitochondria and chloroplasts. Nat Rev Mol Cell Biol **12:** 48–59

Sharma M, Bennewitz B, Klösgen RB (2018a) Dual or not dual? Comparative analysis of fluorescence microscopy-based approaches to study organelle targeting specificity of nuclear-encoded plant proteins. Front Plant Sci **9:** 1350

Sharma M, Bennewitz B, Klösgen RB (2018b) Rather rule than exception? How to evaluate the relevance of dual protein targeting to mitochondria and chloroplasts. Photosynth Res **138:** 335–343

Taylor NL, Heazlewood JL, Day DA, Millar AH (2004) Lipoic acid-dependent oxidative catabolism of α-keto acids in mitochondria provides evidence for branched-chain amino acid catabolism in Arabidopsis. Plant Physiol **134:** 838–848

Torkko JM, Koivuranta KT, Miinalainen IJ, Yagi AI, Schmitz W, Kastaniotis AJ, Airenne TT, Gurvitz A, Hiltunen KJ (2001) Candida tropicalis Etr1p and Saccharomyces cerevisiae Ybr026p (Mrf1′p), 2-enoyl thioester reductases essential for mitochondrial respiratory competence. Mol Cell Biol **21:** 6243–6253

van Wijk KJ, Baginsky S (2011) Plastid proteomics in higher plants: Current state and future goals. Plant Physiol **155:** 1578–1588

Wada H, Shintani D, Ohlrogge J (1997) Why do mitochondria synthesize fatty acids? Evidence for involvement in lipoic acid production. Proc Natl Acad Sci USA **94:** 1591–1596

Wada M, Yasuno R, Jordan SW, Cronan JE Jr., Wada H (2001a) Lipoic acid metabolism in Arabidopsis thaliana: Cloning and characterization of a cDNA encoding lipoyltransferase. Plant Cell Physiol **42:** 650–656

Wada M, Yasuno R, Wada H (2001b) Identification of an Arabidopsis cDNA encoding a lipoyltransferase located in plastids. FEBS Lett **506:** 286–290

Wu GZ, Xue HW (2010) Arabidopsis β-ketoacyl-[acyl carrier protein] synthase I is crucial for fatty acid synthesis and plays a role in chloroplast division and embryo development. Plant Cell **22:** 3726–3744

Wu J, Sun Y, Zhao Y, Zhang J, Luo L, Li M, Wang J, Yu H, Liu G, Yang L, et al (2015) Deficient plastidic fatty acid synthesis triggers cell death by modulating mitochondrial reactive oxygen species. Cell Res **25:** 621–633

Yasuno R, von Wettstein-Knowles P, Wada H (2004) Identification and molecular characterization of the beta-ketoacyl-[acyl carrier protein] synthase component of the Arabidopsis mitochondrial fatty acid synthase. J Biol Chem **279:** 8242–8251

Yasuno R, Wada H (1998) Biosynthesis of lipoic acid in Arabidopsis: Cloning and characterization of the cDNA for lipoic acid synthase. Plant Physiol **118:** 935–943

Yasuno R, Wada H (2002) The biosynthetic pathway for lipoic acid is present in plastids and mitochondria in *Arabidopsis thaliana*. FEBS Lett **517:** 110–114

Zhu H, Gonzalez R, Bobik TA (2011) Coproduction of acetaldehyde and hydrogen during glucose fermentation by *Escherichia coli*. Appl Environ Microbiol **77:** 6441–6450